Article

Ultrafast Excited-State Dynamics of Kynurenine, a UV Filter of the Human Eye

SHERIN, Peter S., *et al*.

Abstract

The excited-state dynamics of kynurenine (KN) has been examined in various solvents by femtosecond-resolved optical spectroscopy. The lifetime of the S1 state of KN amounts to 30 ps in aqueous solutions, increases by more than 1 order of magnitude in alcohols, and exceeds 1 ns in aprotic solvents such as DMSO and DMF, internal conversion (IC) being shown to be the main deactivation channel. The IC rate constant is pH independent but increases with temperature with an activation energy of about 7 kJ/mol in all solvents studied. The dependence on the solvent proticity together with the observation of a substantial isotope effect indicates that hydrogen bonds are involved in the rapid nonradiative deactivation of KN in water. These results give new insight into the efficiency of KN as a UV filter and its role in cataractogenesis.

Reference

SHERIN, Peter S., *et al*. Ultrafast Excited-State Dynamics of Kynurenine, a UV Filter of the Human Eye. *The journal of physical chemistry. B*, 2009, vol. 113, no. 14, p. 4953-4962

DOI : 10.1021/jp900541b

Ultrafast Excited-State Dynamics of Kynurenine, a UV Filter of the Human Eye

Peter S. Sherin,*,† Jakob Grilj,‡ Yuri P. Tsentalovich,† and Eric Vauthey*,‡

International Tomography Center SB RAS, Institutskaya 3a, 630090 Novosibirsk, Russia, and Department of Physical Chemistry, University of Geneva, 30 quai Ernest-Ansermet, CH-1211 Geneva 4, Switzerland

Received: January 19, 2009

The excited-state dynamics of kynurenine (KN) has been examined in various solvents by femtosecond-resolved optical spectroscopy. The lifetime of the S_1 state of KN amounts to 30 ps in aqueous solutions, increases by more than 1 order of magnitude in alcohols, and exceeds 1 ns in aprotic solvents such as DMSO and DMF, internal conversion (IC) being shown to be the main deactivation channel. The IC rate constant is pH independent but increases with temperature with an activation energy of about 7 kJ/mol in all solvents studied. The dependence on the solvent proticity together with the observation of a substantial isotope effect indicates that hydrogen bonds are involved in the rapid nonradiative deactivation of KN in water. These results give new insight into the efficiency of KN as a UV filter and its role in cataractogenesis.

Introduction

The solar light that reaches our eyes after transmission through the atmosphere still contains ultraviolet components with wavelengths >280 nm. In humans and other primates' eyes, UV light below 300 nm is filtered out by the cornea, while most of the 300−400 nm light is absorbed by low-molecular-weight compounds contained in the lens and thus protecting the retina from UV irradiation. These compounds, kynurenine (KN), 3-hydroxykynurenine (3OHKN), 3-hydroxykynurenine *O*-β-D-glucoside (3OHKG), and their derivatives (Chart 1),[1−3] originate from the amino acid tryptophan and absorb UV light in the 300−400 nm spectral region. Kynurenines are weak photosensitizers and redirect the absorbed light energy into benign channels.[4−7] They are characterized by a low fluorescence quantum yield and lifetime,[4] a low triplet yield,[8] a high photochemical stability,[9,10] and, under aerobic conditions, a low singlet oxygen and/or superoxide photogeneration.[6] All these observations point to the existence of a fast $S_1 \rightarrow S_0$ radiationless deactivation.

Nitrogen-heterocyclic and aromatic carbonyl compounds often exhibit very efficient ground-state recovery after optical excitation. One of the proposed mechanisms for a fast nonradiative decay of the lowest singlet excited state is the so-called "proximity effect", which originates from the vibronic interaction between close-lying n,π^* and π,π^* excited states.[11−14] The prevalence of this mechanism depends strongly on the environment because of the sensitivity of the n,$\pi^*-\pi,\pi^*$ energy gap to solvent polarity and hydrogen-bonding ability. Another proposed mechanism involves a repulsive $\pi\sigma^*$ state connecting the lowest singlet excited state to the ground state via conical intersections.[15] A similar mechanism involving a conical intersection between the S_1 and S_0 states was also suggested to account for the subpicosecond fluorescence lifetime of uracil and its derivatives.[16]

The rate of nonradiative $S_1 \rightarrow S_0$ transitions can also be significantly affected by intra- and intermolecular hydrogen bonds. The origin of this effect is the redistribution of the electron density upon excitation, which alters the acidity/basicity of the functional groups of aromatic compounds and changes the strength of solute−solvent interactions.[17−21] In extreme cases, hydrogen bonds may cause intra- and intermolecular proton transfer reactions in the lowest excited state.[17−21] The deactivation via hydrogen-bond-assisted proton transfer has been reported for methyl salicylate,[22] anthraquinones,[23,24] and some other aromatic molecules.[25−30] A fast deactivation of the photoexcited state was also found with *o*-aminoacetophenone (AAP) and its derivatives, whose chemical structures are similar to that of KN.[31,32] It has been shown that internal conversion (IC) is the main decay channel of the S_1 state, and that its rate constant is highly sensitive to the solvent: in polar aprotic solvents, the fluorescence lifetime of AAP exceeds 1 ns, while in polar protic and nonpolar solvents it decreases by one and two orders of magnitude.[31] These effects were explained in terms of proximity effect and hydrogen-bonding interactions between the carbonyl and the amino groups of AAP in nonpolar solvents, and between AAP and protic solvent molecules.

CHART 1

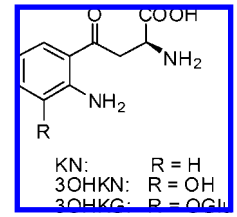

We report here on a detailed investigation of the primary events following UV excitation of KN in solution using femtosecond-resolved optical spectroscopy. The main goals of this work are (i) to study the photophysical properties of the lowest singlet excited state of KN and (ii) to establish the origin of the efficient deactivation of this state. The excited-state dynamics of KN has never been investigated with sufficient time resolution until now, but such a study is crucial for a detailed understanding of the mechanism of UV-protection by kynurenines.

* Corresponding authors. Tel: +7-(383)-330-31-36; fax: +7-(383)-333-13-99; e-mail: sherin@tomo.nsc.ru; (P.S.S.); tel: +41-22-379-65-37, fax: +41-22-379-65-18, e-mail: eric.vauthey@unige.ch (E.V.).
† International Tomography Center SB RAS.
‡ University of Geneva.

10.1021/jp900541b CCC: $40.75
Published on Web 03/18/2009

Experimental Methods

Materials. Kynurenine (KN), 3-hydroxykynurenine (3OHKN), and quinine bisulfate were used as received from Sigma/Aldrich. H_2O was doubly distilled. The other solvents, deuterated water (D_2O), methanol (MeOH), ethanol (EtOH), *N*,*N*-dimethylformamide (DMF), and dimethyl sulfoxide (DMSO) were used as received from Fluka. The aqueous solutions were not buffered and their pH was controlled using a Mettler Toledo FG2/EL2 pH meter.

Steady-State Measurements. Steady-state absorption and fluorescence spectra were measured with a Cary 50 (Varian) spectrophotometer and a Cary Eclipse (Varian) fluorometer, respectively. All fluorescence spectra were corrected for the wavelength-dependent sensitivity of the detection. A cryostat unit (Optistat DN, Oxford Instruments) was used for the fluorescence measurements in the low-temperature range. All solutions were deoxygenated by argon bubbling for 15 min prior to measurements, capped, and sealed with parafilm. The fluorescence quantum yields were determined relative to a 1.0 N H_2SO_4 aqueous solution of quinine bisulfate, for which the fluorescence quantum yield ($\Phi_{fl} = 0.546$ at 365 nm excitation) is known.[33] For all measurements, a 10 × 10 mm^2 quartz cell was used and the absorbance of the samples was below 0.1 at the absorption maximum.

Time-Resolved Fluorescence Measurements. The early fluorescence dynamics were measured using the fluorescence up-conversion setup described in detail elsewhere.[34] Briefly, part of the output of a mode locked Ti:sapphire laser (Spectra Physics "Tsunami") was frequency-doubled and used to excite the sample at 400 nm. The fluorescence was gated by sum-frequency mixing with the fundamental of the oscillator output. The up-converted UV photons were directed into a monochromator and detected by a photomultiplier with photon counting electronics. The sample solutions were kept in a 1.0 mm thick spinning cell. The KN concentration was adjusted so that the absorbance of the sample was around 0.15 at the excitation wavelength. The full width at half-maximum (fwhm) of the instrument response function was around 210 fs. Time profiles longer than 1 ns were measured using the time-correlated single photon counting (TCSPC) unit described in ref 35. A pulsed laser diode at 395 nm with a repetition rate of 40 MHz was used for excitation. A 10 × 10 mm^2 quartz cell was used and the sample absorbance at 395 nm was about 0.1. The fwhm of the instrument response function was around 200 ps. All time-resolved measurements were carried out at room temperature.

Transient Absorption Measurements. The experimental setup for transient absorption (TA) has been described in detail elsewhere.[36] Excitation was performed at 400 nm using the frequency-doubled output of a standard 1 kHz amplified Ti:sapphire system (Spectra-Physics). The pump intensity on the sample was around 3 μJ. Probing was achieved with a white-light continuum obtained by focusing a small fraction of the 800 nm pulses in a CaF_2 plate. The polarization of the probe pulses was at magic angle relative to that of the pump pulses. All spectra were corrected for the chirp of the white light probe pulses. The fwhm of the instrument response function was ca. 200 fs. The sample solutions were placed in a 1 mm thick quartz cell where they were continuously stirred by N_2-bubbling. Their absorbance at the excitation wavelength was around 0.15.

Triplet Quantum Yield Measurements. The triplet quantum yields of KN (Φ_T) were measured with a laser flash photolysis setup, a detailed description of which has been published earlier.[37,38] The solutions, located in a 10 × 10 mm^2 cell, were irradiated with a Quanta-Ray LAB-130-10 Nd:YAG laser (pulse duration 8 ns; 355 nm; pulse energy up to 150 mJ). The spot size of the laser beam at the cell entrance was 2.5 × 8 mm^2. The monitoring system included a DKSh-150 xenon short-arc lamp connected to a high-current pulser, a homemade monochromator, a 9794B photomultiplier Electron Tubes Ltd., and a LeCroy 9310A digitizer. The monitoring light, concentrated in a 2.5 × 1 mm^2 rectangle, passed through the cell along the front window. In all experiments, the excitation optical length was 1 mm, and the monitoring optical length was 8 mm. All solutions were bubbled with argon for 15 min prior to and during irradiation.

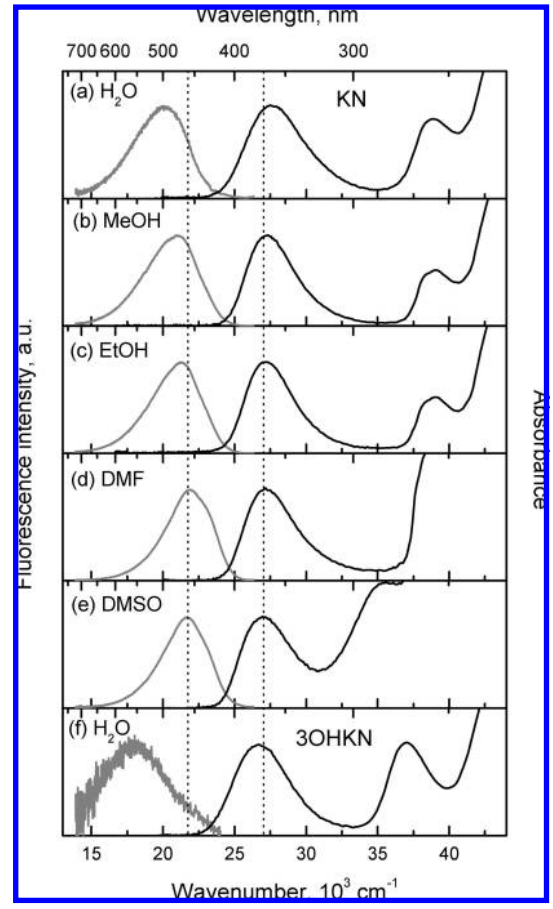

Figure 1. Steady-state absorption and fluorescence spectra of KN in (a) H_2O, pH 6.6, (b) MeOH, (c) EtOH, (d) DMF, and (e) DMSO and of (f) 3OHKN in H_2O, pH 6.6 at room temperature.

TABLE 1: Absorption Maximum, λ_{max}^{abs}, Molar Absorption Coefficient, ε_{max}[a] at λ_{max}^{abs}, Fluorescence Maximum, λ_{max}^{fl}, and Stokes Shift, $\Delta\nu$, of KN in Various Solvents and of 3OHKN in H_2O at Room Temperature

compound	solvent	λ_{max}^{abs}, nm	ε_{max}, M^{-1} cm^{-1}	λ_{max}^{fl}, nm	$\Delta\nu$, 10^3 cm^{-1}
KN	H_2O	361	4850	500	7.7
	MeOH	367	6100	474	5.9
	EtOH	369	6750	469	5.7
	DMF	366	5900	457	5.3
	DMSO	368	6500	461	5.3
3OHKN	H_2O	375	4200	557	8.7

[a] Error on ε_{max}: 5%.

Results

Steady-State Measurements. Figure 1 shows absorption and fluorescence spectra of KN in various solvents at room tem-

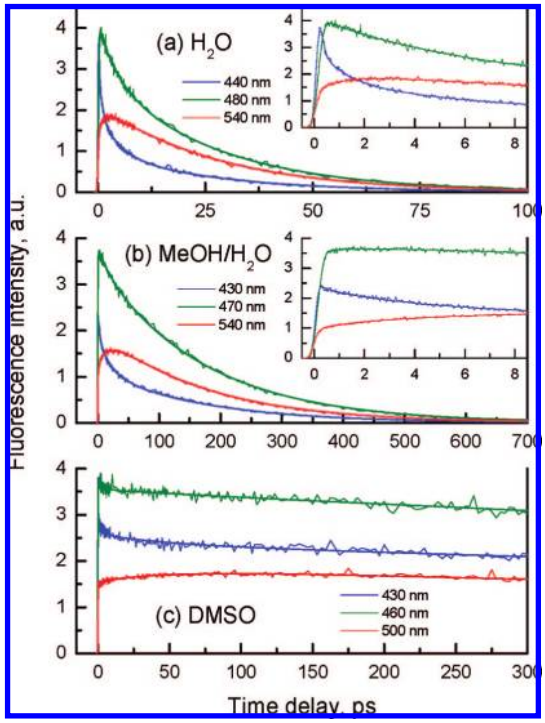

Figure 2. Time profiles of the fluorescence intensity measured with KN in (a) H_2O, pH 6.6, (b) MeOH/H_2O 10/1 (v/v) mixture, and (c) DMSO. The smooth lines present the best multiexponential fits. Inset: early dynamics at the same wavelengths.

perature. KN exhibits a minor blue shift of the absorption band and a marked red shift of the fluorescence band by going from aprotic to protic solvents. The absorption (λ_{max}^{abs}) and fluorescence (λ_{max}^{fl}) maxima, Stokes shifts ($\Delta\nu$), and extinction coefficients at the corresponding absorption maxima (ε_{max}) of KN are listed in Table 1. The relatively large Stokes shift of the fluorescence and of the first absorption band can be accounted for by the intramolecular charge transfer character of the transition introduced by the amino-substituent on the aromatic ring. On the other hand, the monotonic red shift of KN fluorescence band in protic solvents might be interpreted as participation of intermolecular hydrogen bonds in the stabilization of the S_1 state.

Time-Resolved Measurements. The temporal evolution of KN fluorescence intensity has been measured in H_2O (pH 6.6), MeOH/H_2O 10/1 (v/v) mixture, and in DMSO at 10 equidistant wavelengths from 420 to 580 nm throughout the emission band over different time windows up to 700 ps. Figure 2 shows fluorescence times profiles recorded at the high-energy side, the center, and the low-energy side of the emission band. The amplitudes of the time profiles measured at different wavelengths where rescaled with the factor, $F(\lambda)$:

$$F(\lambda) = \frac{S(\lambda)}{\int_0^\infty D(\lambda, t)\, dt} \quad (1)$$

where $S(\lambda)$ is the steady-state fluorescence intensity and $D(\lambda,t)$ is the measured fluorescence time profile. The fast signal decay at the blue side and the corresponding rise at the red side of the band are characteristic features of emission during solvent relaxation and correspond to a red shift of the band, a so-called dynamic Stokes shift. This shift can be more clearly seen from the reconstructed time-resolved emission spectra presented in Figure 3. After this process, the shape of the fluorescence spectrum remains unchanged and coincides with the steady-state emission spectrum (thick line in Figure 3).

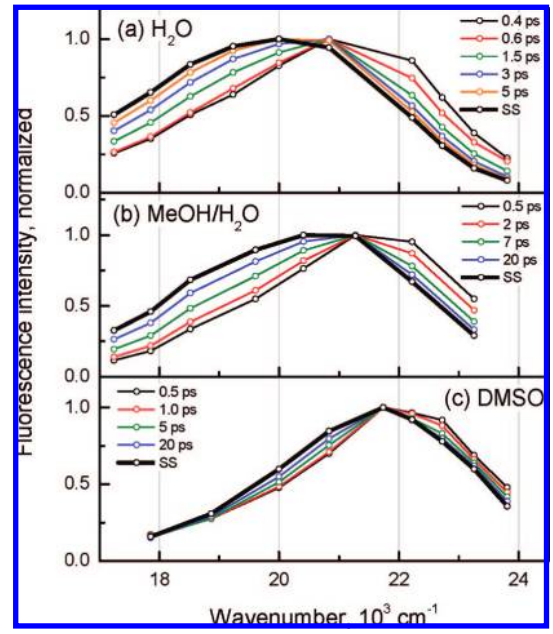

Figure 3. Intensity normalized time-resolved fluorescence spectra of KN in (a) H_2O pH 6.6, (b) binary mixture MeOH/H_2O 10/1 (v/v), and (c) DMSO. The bold lines are the steady-state fluorescence spectra.

The experimental data were analyzed globally using a sum of exponentials convolved with a Gaussian-like instrument response function as described in details in refs 39 and 40. A good agreement between experimental and calculated data in all three solvents was obtained with three exponentials. The best fits, shown by smooth lines in Figure 2, were obtained with the time constants, τ_1 to τ_3, listed in Table 2. The latter reveals a significant slowing down of the fluorescence dynamics by going from H_2O to MeOH/H_2O mixture (10/1, v/v) and DMSO.

Figure 4 depicts the spectra of the amplitude factors associated with the three time constants, $A_1(\lambda)$, $A_2(\lambda)$, and $A_3(\lambda)$, obtained from the global fit. Positive values correspond to a decay and negative ones to a rise of the intensity. In all three media, the spectra associated with the fast components, $A_1(\lambda)$ and $A_2(\lambda)$, exhibit a similar shape indicative of a decay on the high-energy side and a rise on the low-energy side of the emission band. These components can thus be attributed predominantly to a dynamic Stokes shift. The amplitude spectrum, $A_3(\lambda)$, associated with the largest time constant almost coincides with the steady-state emission spectrum (thin gray line). This indicates that this time constant corresponds to the decay of the excited-state population and thus τ_3 can be identified as the lifetime of the lowest singlet excited state of KN. Table 2 shows that τ_3 exhibits the strongest solvent dependence: it increases by 2 orders of magnitude from H_2O to DMSO. The τ_1 and τ_2 values increase as well, but to a lesser extent.

TA spectra recorded at different time delays after 400 nm excitation of KN in aqueous solution (pH 6.6) are shown in Figure 5a. Immediately after excitation, a TA band with a maximum at 570 nm is observed. During the first 10 ps, this band shifts from 570 to 550 nm, the initial dip at about 470 nm vanishes and the positive TA signal above 600 nm becomes negative. At later times, a monotonic decay of the TA signal without any significant spectral change can be observed. The positive signal can be attributed to $S_1 \rightarrow S_n$ absorption and the negative signal to $S_1 \rightarrow S_0$ stimulated emission. The initial spectral dynamics can be ascribed to the time-dependent Stokes shift of the stimulated emission band. Indeed, Figure 1a shows that the fluorescence band overlaps with the $S_1 \rightarrow S_n$ absorption

TABLE 2: Time Constants Obtained from the Global Analysis of the Fluorescence and TA Dynamics, τ_i, Fluorescence Quantum Yield, Φ_F, and Radiative Rate Constant, k_F, of KN and 3OHKN in Various Solvents at Room Temperature (Standard Error 10%)

compound	solvent	τ_1, ps	τ_2, ps	τ_3, ps	Φ_F, 10^{-2}	k_F, s^{-1}
KN	H_2O (pH 1.9)	0.9	4.6	29.4	0.079	2.7×10^7
	H_2O (pH 6.6)	0.9	4.5	27.1	0.082	3.0×10^7
		(1.0)[a]	(5.4)[a]	(25.8)[a]		
	H_2O (pH 11)	0.9	4.4	30.5	0.101	3.3×10^7
	D_2O	1.2	6.6	43.5	0.135	3.1×10^7
	MeOH/H_2O (10/1)	2.6	19.6	172	0.51	3.0×10^7
		(2.0)[a]	(18.5)[a]	(161)[a]		
	MeOH	–	–	240[b]	0.79	3.3×10^7
	EtOH	–	–	480[b]	2.3	4.8×10^7
	DMF	–	–	1390[b]	5.3	3.8×10^7
	DMSO	3.3	41.4	2260	9.0	4.0×10^7
		(4.3)[a]	(51.8)[a]	(2440)[a]		
3OHKN	H_2O (pH 6.6)	0.6	3.0	9.6	0.016	1.6×10^7
	D_2O	0.9	6.2	22.9	0.025	1.1×10^7

[a] Obtained from the global fit analysis of TA time profiles (see text). [b] Obtained from the TCSPC measurements (see text).

spectrum over almost the whole wavelength region investigated, whereas the time-resolved fluorescence measurements point to a dynamic Stokes shift from 480 to 500 nm (about 850 cm^{-1}) occurring on the same time scale as the shift of the TA band from 570 to 550 nm (about 650 cm^{-1}). However, an intrinsic initial blue shift of the $S_1 \rightarrow S_n$ absorption band could as well contribute to the observed spectral dynamics.

A global analysis of the TA spectra was performed with the sum of three exponential functions and gave time constants very similar to those obtained from the fluorescence measurements (Table 2); the associated amplitude spectra, $B_1(\lambda)$, $B_2(\lambda)$, and $B_3(\lambda)$, being shown in Figure 6a. Those associated with the fast components, $B_1(\lambda)$ and $B_2(\lambda)$, are similar in shape to the $A_1(\lambda)$ and $A_2(\lambda)$ spectra but with opposite signs (Figure 4a). These two time constants can be assigned to the dynamics Stokes shift of the stimulated emission, the opposite signs of the amplitudes of the associated spectra being due the negative intensity of the stimulated emission in a TA spectrum. On the other hand, the $B_3(\lambda)$ spectrum resembles the TA spectra after the initial spectral dynamics and the associated time constant can be interpreted as the decay time of the S_1 state population. The TA results are fully consistent with the time-resolved fluorescence data.

TA spectra recorded with KN in MeOH/H_2O mixture (10/1, v/v) and DMSO are presented in Figure 5b,c. The early dynamics in these solvents is qualitatively very similar to that found in water. Furthermore, the TA intensity decays subsequently without any appreciable spectral changes, like in water. The spectral dynamics can be also explained in the terms of a red shift of the stimulated emission. In MeOH/H_2O mixture and in DMSO, the fluorescence emission band is blue-shifted compared to water (Figure 1b,e) explaining the absence of the negative signal at $\lambda > 600$ nm found in aqueous solutions.

The global analysis of the TA spectra in MeOH/H_2O mixture and DMSO, performed as described above, yielded time constants very similar to those obtained from the fluorescence data (Table 2). The decay associated spectra presented in Figure 6b,c are like those in H_2O. The only exception is $B_1(\lambda)$, which exhibits a double maximum in the positive part of the spectrum in both MeOH/H_2O mixture and DMSO. This shape is most probably due to the superposition of different phenomena such as the solvent and vibrational relaxation of the S_1 state. The occurrence of vibrational relaxation, which results to a narrowing of the absorption band, is supported by the location of the $B_1(\lambda)$ maxima at the edges of the TA band.[41] Contribution of vibrational relaxation to the early spectral dynamics observed in the time-resolved fluorescence measurement cannot be excluded; however, the associated spectral narrowing might be hidden by the dynamic Stokes shift.

It should be emphasized that after the decay of the $S_1 \rightarrow S_n$ TA band, no absorbance from any other species could be detected over the whole spectral window in all solvents investigated. This indicates that the only transient that is observed in both time-resolved fluorescence and absorption measurements is the first singlet excited state of KN. Figure 7 depicts the temporal evolutions of fluorescence and TA intensity at the maxima of the corresponding bands in the three solvents used, which thus mainly reflect the decay of the S_1 state population.

In order to study the nature of the deactivation process, the same absorption and fluorescence experiments were carried out with KN in H_2O at pH 1.9 and 11 and in D_2O. The characteristic time constants obtained from the analysis of the fluorescence data as described above are listed in Table 2.

In acidic and basic solutions, no noticeable changes in the excited-state dynamics were found (data not shown). The time constants obtained from triexponential analysis are approximately the same in acidic, neutral, and basic solutions (Table 2). Thus, it can be concluded that the dynamics of KN excited state is mostly pH independent.

In deuterated water, the excited-state dynamics is slowed down compared to water, whereas the shapes of the fluorescence and TA spectra remain the same. The temporal evolution of the fluorescence and TA intensity at the band maxima in H_2O and D_2O are presented in Figure 7. Table 2 shows that all three time constants increase on average by a factor of 1.5. This observation points to a substantial participation of hydrogen bonds in the ultrafast deactivation of KN excited state.

The early excited-state dynamics of KN could not be studied in MeOH, EtOH, and DMF, because of the low solubility of KN in these solvents. However, TCSPC fluorescence measurements could be performed. The KN emission exhibits an exponential decay in all these solvents with a time constant that is wavelength independent in the 420−650 nm region. The resulting fluorescence lifetimes of KN corresponding to the S_1-state lifetimes τ_3 and are summarized in Table 2.

Quantum Yield Measurements. The fluorescence quantum yields, Φ_F, of KN in various solvents are summarized in Table 2. The increase of Φ_F from protic to aprotic solvents reflects the increase of fluorescence lifetime.

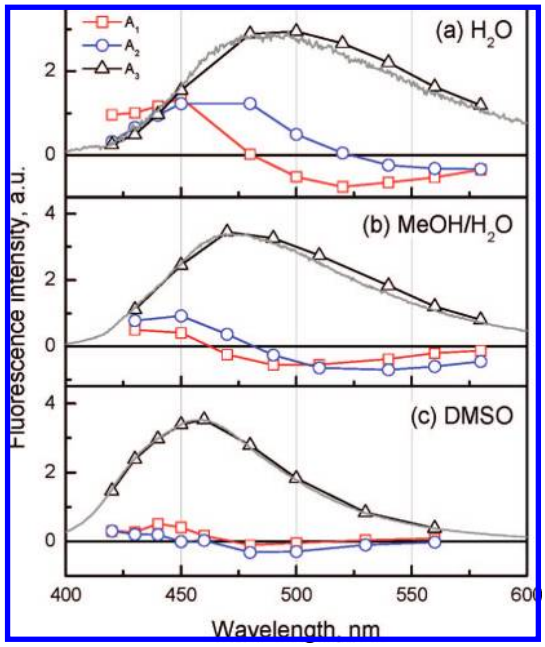

Figure 4. Decay-associated amplitude spectra obtained from the global analysis of the fluorescence time profiles measured with KN in (a) H_2O pH 6.6, (b) binary MeOH/H_2O 10/1 (v/v) mixture, and (c) DMSO. The gray lines are the steady-state fluorescence spectra.

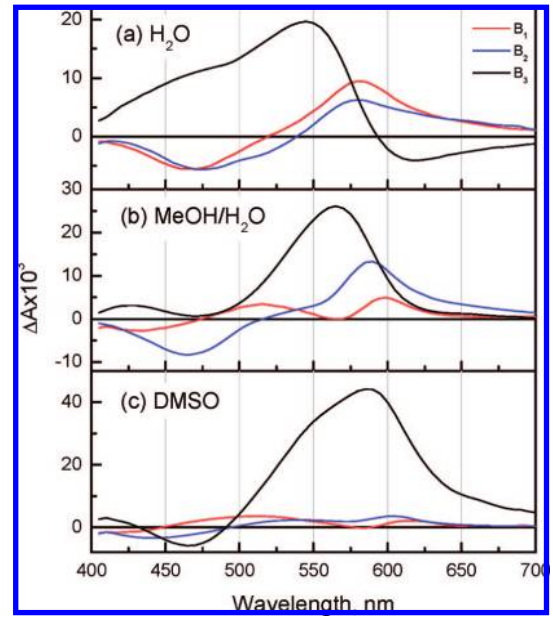

Figure 6. Decay-associated amplitude spectra obtained from the global analysis of TA spectra of KN in (a) H_2O pH 6.6, (b) MeOH/H_2O 10/1 (v/v) mixture, and (c) DMSO.

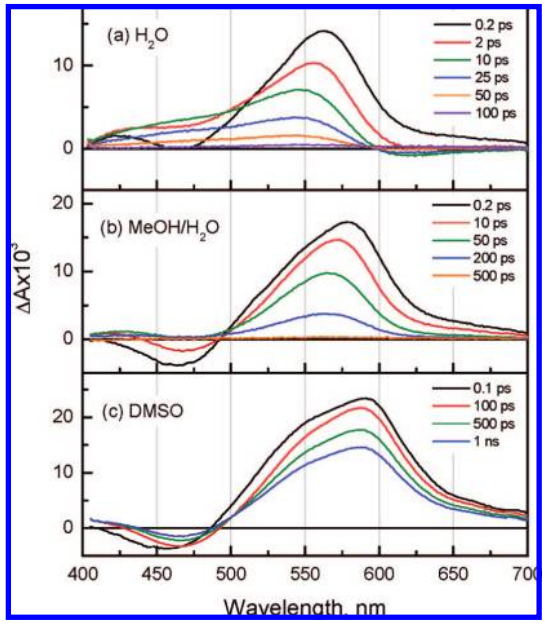

Figure 5. TA spectra recorded at different time delays after excitation of KN in (a) H_2O, (b) MeOH/H_2O 10/1 (v/v) mixture, and (c) DMSO.

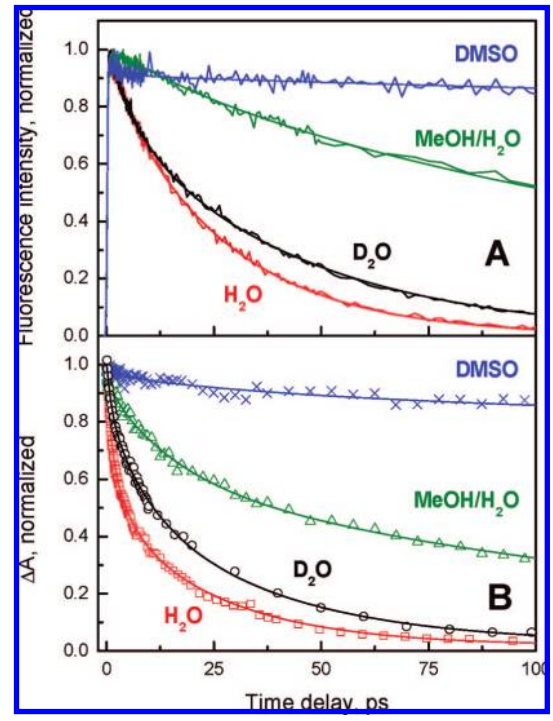

Figure 7. (A) Fluorescence time profiles recorded with KN at the emission maximum and (B) time profiles of TA intensity of KN at the band maximum.

The triplet state quantum yields, Φ_T, of KN in various solvents were measured by laser photolysis with a procedure described in detail earlier.[10] The absorbance of the triplet KN was measured at 430 nm, the maximum of the triplet state absorption band.[8] The contribution of the triplet state to the total transient absorption at this wavelength was separated by performing the measurements under argon and under oxygen. The residual absorption at 430 nm corresponds to KN radicals formed via biphotonic ionization with the second photon absorbed by KN in the triplet state;[42] this process was also taken into account in the triplet quantum yield calculations. The calculations were performed presuming that the absorption coefficients of KN triplet state and radicals at 430 nm[42] do not depend on the solvent, and using the previously reported value[8] of $\Phi_T(H_2O) = 0.018$ as reference. The results of the calculations listed in Table 3 show an apparent correlation between the triplet yield and the rate constant of internal conversion.

The fluorescence and triplet quantum yields of KN were measured in H_2O/DMSO binary mixtures as well. Figure 8 shows these yields plotted against the molar fractions of H_2O and DMSO. Both yields exhibit a monotonic decrease with the increase of H_2O molar fraction, the most pronounced decrease

TABLE 3: Kamlet−Taft's Solvatochromic Parameter, α,[44,45] Triplet and IC Quantum Yields, Φ_T and Φ_{IC}, and ISC and IC Rate Constants, k_{ISC} and k_{IC}, of KN and 3OHKN in Various Solvents at Room Temperature (Standard Error 10%)

compound	solvent	α	Φ_T, 10^{-2}	k_{ISC}, s^{-1}	Φ_{IC}, 10^{-2}	k_{IC}, s^{-1}
KN	H_2O (pH 1.9)		1.7	5.8×10^8	98.2	3.3×10^{10}
	H_2O (pH 6.6)	1.17	1.8	6.6×10^8	98.1	3.6×10^{10}
	H_2O (pH 11)		1.9	6.2×10^8	98.0	3.2×10^{10}
	D_2O		2.2	5.1×10^8	97.7	2.3×10^{10}
	MeOH/H_2O (10/1)		3.1	1.8×10^8	96.4	5.6×10^9
	MeOH	0.93	5.2	2.2×10^8	94.0	3.9×10^9
	EtOH	0.83	7.4	1.5×10^8	90.3	1.9×10^9
	DMF	0	25.0	1.8×10^8	69.7	5.1×10^8
	DMSO	0	33.4	1.5×10^8	57.6	2.6×10^8
3OHKN	H_2O (pH 6.6)	1.17	<0.5[a]	$<5.2 \times 10^8$	>99.5	$>10.4 \times 10^{10}$
	D_2O		<0.5[a]	$<5.2 \times 10^8$	>99.5	$>4.4 \times 10^{10}$

[a] Taken from ref 10.

TABLE 4: Activation Energies E_{NR} and Ratios A_{NR}/k_F for the Nonradiative Rate Constant of KN in Various Solvents

solvent	E_{NR}, kJ/mol	$\ln(A_{NR}/k_F)$
MeOH	6.6 ± 0.4	7.5 ± 0.7
EtOH	7.2 ± 0.4	6.7 ± 0.7
DMF	8.2 ± 0.4	6.1 ± 0.6

of Φ_F being observed at $\chi_{H_2O} > 0.7$. It should be noted that the nature of the solvation shell with H_2O/DMSO mixture does not show a linear dependence on the ratio of components but depends on the microscopic structure of the H_2O/DMSO mixture. It has been recently shown that compounds such as 2-butanol, cyclopentanol, cyclohexane, and phenol in H_2O/DMSO are predominantly solvated by water clusters at $\chi_{H_2O} > 0.9$ and predominantly by DMSO clusters at $\chi_{H_2O} < 0.9$.[43] The experimental results presented in Figure 8 reveal that KN is not predominantly solvated by DMSO clusters in the range $0 < \chi_{H_2O} < 0.7$, otherwise the fluorescence and triplet yields would remain unchanged in this region. This might be due to intermolecular hydrogen-bond interactions between KN and water molecules. The dependence of Φ_F on the composition of the solvent mixture allows a value of $\chi_{H_2O} = 0.7$ to be suggested as a border, dividing the regions where DMSO and water molecules represent the major component of KN solvation shell.

The obtained Φ_F and Φ_T values were used for calculating the rate constants of the main excited-state decay channels: fluorescence, intersystem crossing, and internal conversion. The radiative rate constant k_F was evaluated from the ratio of the fluorescence quantum yield Φ_F to the fluorescence lifetime τ_3:

$$k_F = \Phi_F/\tau_3 \quad (2)$$

The k_F values of KN amount to about $(3-4) \times 10^7$ s^{-1} independently of the solvent.

The nonradiative decay channels of the S_1 state can include ionization, intersystem crossing (ISC), and internal conversion (IC). Ionization can be neglected because of the absence of a signal from the solvated electron in the long-wavelength region of the TA spectra (Figure 5). Thus, the main nonradiative decay channels are ISC and IC; the rate constants of these processes have been estimated according the following expressions:

$$k_{ISC} = \Phi_T/\tau_3 \quad (3)$$

$$k_{IC} = (1 - \Phi_F - \Phi_T)/\tau_3 \quad (4)$$

It can be seen from Table 3 that k_{ISC} exhibits a 4-fold increase from aprotic to protic solvents. Returning to Figure 8, the differences in the dependencies of Φ_F and Φ_T on the composition of H_2O/DMSO mixture might be attributed to the solvent independence of the k_F value and the solvent dependence of k_{ISC}. The value of k_{IC} increases by more than 2 orders of magnitude from DMSO to H_2O. The drastic increase of k_{IC} in protic solvents corresponds to the increase of hydrogen-bonding ability of the solvent, which can be quantified with the Kamlet−Taft's solvatochromic parameter α[44,45] shown in Table 3.

Temperature Dependence of the Fluorescence. The influence of temperature on the fluorescence intensity and spectra of KN was studied in MeOH, EtOH, and DMF. The measurements were carried out from room temperature down to the freezing point of the solvent. The fluorescence spectra of KN in EtOH at different temperatures are presented in Figure 9, the same spectra after intensity normalization being shown in the inset. The decrease of temperature leads to an increase of the fluorescence intensity and to a change of band shape. Figure 10 shows the temperature dependence of the center of gravity of KN fluorescence spectra in MeOH, EtOH, and DMF. In DMF, this parameter is temperature independent, whereas in alcohols it shows a blue shift, which occurs mainly in the 160−220 K range. The reason for the blue shift and the changes in spectral shape is most likely the high viscosity of alcohols at low temperatures, which leads to a slowing down of solvent motion. Thus, emission mostly occurs from a thermally nonrelaxed singlet excited state. This effect does not appear in DMF because the fluorescence lifetime remains substantially larger than the solvation time even at low temperature.

The fluorescence quantum yield of KN, Φ_F, can be expressed as

$$\Phi_F = \frac{k_F}{k_F + k_{ISC} + k_{IC}} = \frac{k_F}{k_F + k_{NR}} \quad (5)$$

where $k_{NR} = k_{ISC} + k_{IC}$ is the rate constant of nonradiative transitions. We can assume that the temperature dependence of k_{NR} can be expressed according to an Arrhenius law

$$k_{NR} = A_{NR} \exp\left(-\frac{E_{NR}}{RT}\right) \quad (6)$$

From (5) and (6) a linear relationship can be obtained:

$$\ln\left(\frac{1}{\Phi_F} - 1\right) = \ln\left(\frac{A_{NR}}{k_F}\right) - \frac{E_{NR}}{RT} \quad (7)$$

Figure 11 shows a plot of $\ln(1/\Phi_F - 1)$ vs $1/T$ in MeOH, EtOH and DMF. The linear fit yields the activation energies E_{NR} and $\ln(A_{NR}/k_F)$, which are collected in Table 4. Since the contribution of k_{ISC} to k_{NR} is of minor importance (Table 3), the obtained value of E_{NR} can be interpreted as the activation

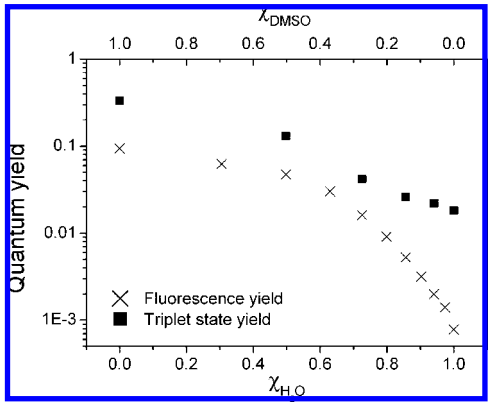

Figure 8. Fluorescence and triplet quantum yields of KN as a function of the molar fraction of H_2O and DMSO in H_2O/DMSO binary mixtures at room temperature (standard errors: 10% for fluorescence and 20% for triplet yield measurements).

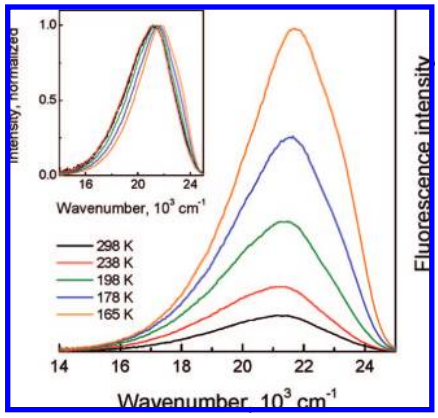

Figure 9. Steady-state fluorescence spectra of KN in EtOH recorded at different temperatures. Inset: same spectra after intensity normalization.

energy for k_{IC}. Interestingly, E_{NR} depends only weakly on the solvent and is smaller than the activation energies associated with solvent viscosity: 12.8 kJ/mol for MeOH and 13.1 kJ/mol for EtOH.[46] These small activation energies are in total agreement with the ultrafast nonradiative decay of KN excited states.

Study of a Related Compound: 3OHKN. The molecule 3OHKN is characterized by a very low fluorescence quantum yield and a short fluorescence lifetime in aqueous solution, previous attempts to measure these quantities having been unsuccessful.[4,47] The higher sensitivity and time resolution of the equipment used here allowed these values to be determined. The steady-state absorption and fluorescence spectra of 3OHKN in aqueous solution are presented in Figure 1f. Both the absorption and the fluorescence bands of 3OHKN are red-shifted relative to those of KN. This shift should be attributed to the presence of the hydroxyl electron-donating group, which lowers the energy of the π,π^* transition. The fluorescence quantum yield of 3OHKN in H_2O is the smallest among all the systems studied (Table 2).

The time-resolved absorption and fluorescence experiments were carried out with 3OHKN in H_2O (pH 6.6) and D_2O. The TA spectra exhibit the same features that were observed with KN: a blue shift of the band followed by a monotonic intensity decay (data not shown). As shown in Table 2, the shorter time constants do not differ very much from those measured with KN, but τ_3 is 3 times smaller. It can be concluded that the introduction of the electron-donating group in the aromatic

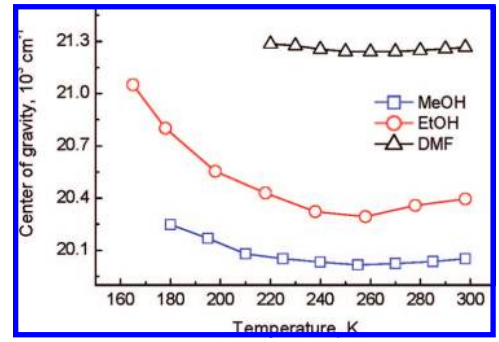

Figure 10. Temperature dependence of the center of gravity of the fluorescence spectra of KN in MeOH, EtOH, and DMF.

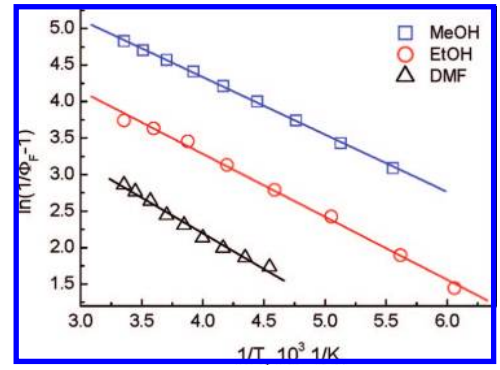

Figure 11. Plots of $\ln(1/\Phi_F-1)$ vs $1/T$ of KN in different solvents and best linear fits.

system markedly accelerates the decay of the singlet state. Apparently, the hydroxyl group is also responsible for more pronounced isotope effect: $\tau_3(D_2O)/\tau_3(H_2O) \sim 2.4$ in the case of 3OHKN.

Discussion

Early Dynamics of KN in the Singlet Excited State. The first electronic transition is characterized by a charge-transfer character introduced by the amino group on the phenyl ring, hence the large Stokes shift of the fluorescence. The time-dependent Stokes shifts shown in Figures 3 and 5 reflect mainly the solvent relaxation dynamics around KN in the S_1 state. Solvent relaxation in aqueous solutions has been shown to be biphasic.[48,49] The initial stage corresponds to the inertial solvent motion—small motion of the solvent molecule or part of it in its own free volume—and is characterized by a time constant of about 150 fs.[48,49] The second stage is associated with the diffusive reorientational motion of the solvent molecule and takes place with a time constant of about 1 ps.[48,49] Given the instrument response functions of about 200 fs, the inertial solvent motion cannot be resolved, whereas the observed $\tau_1 = 0.9$ ps can be rather safely attributed to the diffusive motion of water molecules. The τ_1 values, obtained in other solvents and summarized in Table 2, are also in satisfactory agreement with the solvation times reported in the literature.[48−50] The second time constant, τ_2, is tentatively attributed to structural relaxation of KN in the excited state. Conformational relaxation of a tripeptide has been shown to give rise to slow dynamic Stokes shift components.[51] It should be noted that τ_2 does not exhibit a clear viscosity dependence: it is smaller in H_2O ($\eta_{H_2O} = 0.890$ cP at 25 °C) than in the less viscous MeOH ($\eta_{MeOH} = 0.544$ cP at 25 °C) but is the largest in the more viscous DMSO ($\eta_{DMSO} = 1.987$ cP at 25 °C). However, as H-bonds clearly play a

crucial role in the deactivation of KN in the S_1 state, this apparent lack of a trend might be due to the fact that only solvents with similar proticity should be compared.

Mechanism Responsible for the Ultrafast Internal Conversion. The results obtained point to a very fast decay of KN S_1 state population, with IC as the main channel. The IC rate constant is highly sensitive to the nature of the solvent: it increases by more than 100 times from aprotic to protic solvents. The slowing down of the dynamics in deuterated water points to a direct involvement of the hydrogen bonds in this ultrafast deactivation. A strong influence of the local environment on the rate of nonradiative decay was also reported for many nitrogen-heterocyclic and aromatic carbonyl compounds.[11−14,52] For example, the IC of *o*-aminoacetophenone, which is structurally similar to KN, has been shown to be very fast in nonpolar solvents, and to be drastically slower in polar aprotic solvents.[31,32] This behavior was attributed to the proximity effect.[11−14,52] However, this effect cannot account for the increase of the IC rate constant in protic solvents found here with KN. H-bonding is known to lead to an increase of the n,π^* transition energy, and to a decrease of the of π,π^* transition energy,[53] thus to a larger n,$\pi^*-\pi,\pi^*$ energy gap. According to the proximity effect model, this would results to a slowing down of IC in protic solvents, contrary to the experimental findings. The marked acceleration of IC in 3OHKN compared with KN is also against the proximity effect hypothesis as substitution of a hydrogen by an electron-donating group leads to an increase of the n,$\pi^*-\pi,\pi^*$ energy gap.[54] Finally, the observed temperature dependence is too weak to be attributed to the proximity effect. Activation energies in the range of 1300−1900 cm^{-1} (15.6−22.8 kJ/mol) have been reported for molecules like quinoline and isoquinoline in ethanol, which undergo IC via this effect.[55−57]

The most plausible explanation for the fast IC in protic solvents is the hydrogen-bonding interactions between KN in the S_1 state and the solvent molecules. Excitation of KN results in an increase of the electron density on the carbonyl oxygen. This augments the acidity of the amino group and the basicity of the carbonyl group, which in turns leads to an enhancement of their hydrogen bonding ability. The continuous red shift of KN fluorescence from aprotic to protic solvents supports the involvement of intermolecular hydrogen bonds in the stabilization of the S_1 state. The stretching vibrations of the hydrogen bonds act as accepting modes for the $S_1 \rightarrow S_0$ nonradiative transition and thus the electronic energy dissipates through the hydrogen bonds as vibrational energy. A similar mechanism of fluorescence quenching in ethanol was reported for aminoanthraquinones and aminofluorenones.[17−19] The increase of the hydrogen bonding ability from EtOH to H_2O induces stronger intermolecular hydrogen bonding interactions that results in the acceleration of S_1 state decay. The observed isotope effect ($k_{IC}^{H_2O}/k_{IC}^{D_2O} = 1.5$) strongly supports this mechanism.

In an extreme case, the charge redistribution in the excited KN could lead to a situation where the amino group becomes more acidic, and the carbonyl group more basic than the solvent. In this case, an intermolecular proton transfer may take place as depicted in Scheme 1. The absence of the resulting intermediate in the TA spectra does not allow this mechanism to be totally refuted as it could be due to a very fast decay of this species by back proton transfer to the original ground state of KN.

The occurrence of excited-state intramolecular proton transfer (ESIPT) should also be considered. Indeed, an intramolecular hydrogen bond can be formed between the amino and carbonyl groups of KN. However, in previous reports on ESIPT-induced

SCHEME 1

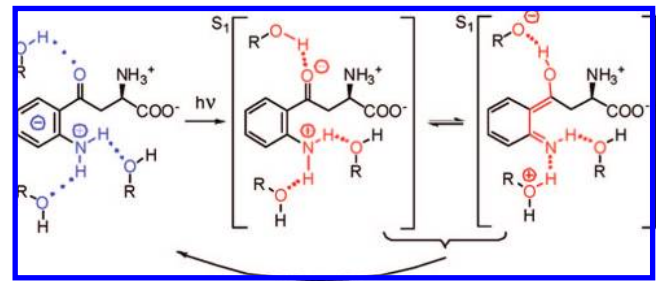

deactivation of methyl salicylate[22] and diaminoanthraquinone,[23,24] the fast fluorescence decay observed was solvent independent. The strong solvent dependence observed here with KN can be attributed to the disruption of the intramolecular hydrogen bonding in protic solvents, which thus inhibits ESIPT.

Finally, it should be emphasized that the charge-transfer character of the S_1 state associated with the redistribution of charge from the amino group lone pair to the aromatic ring is crucial for the function of KN as a UV filter. Protonation of the amino group in highly acidic medium (pH 0.1) suppresses this transition and completely changes the photophysics of KN. In this case, the triplet yield of about unity[8] points to ISC as the main decay channel of the singlet excited state.

Biological Relevance. Because of the low yield of reactive species (triplet states and radicals), kynurenines are very efficient UV filters, protecting the lens and the retina from photodamages. Nevertheless, thermal degradation of these UV filters may result in a modification of the lens proteins.[58,59] Three of them, KN, 3OHKN, and 3OHKG, are unstable under physiological conditions and can undergo spontaneous deamination,[9,60] the deaminated kynurenines binding to lens proteins.[61−64] With age, the accumulation of these modifications changes the properties of the lens proteins: they become colored, fluorescent, and insoluble.[4,5,65,66] In oxidative conditions, the age-related changes may result in an opacification of the human lens and to the development of age-related nuclear cataract.[59] It has recently been reported that the irradiation of bovine lens proteins modified by kynurenines gives rise to peroxide generation mediated by singlet oxygen.[67,68] It has been emphasized that the peroxide generation comes from the change of photochemical activity of UV filters upon binding to protein molecules; in other words, kynurenines in a protein-bound state are more efficient photosensitizers than the free ones. The results of the present work shed some light on the mechanisms of these changes.

In the human lens, the UV filters are mainly present as free molecules that can diffuse in the hydrophilic and highly ordered medium. The incorporation of these molecules into the hydrophobic structure of the lens proteins changes the character of the local environment from protic to aprotic, which, as shown by the present results, drastically increases the lifetime of the singlet excited state and the yield of the reactive triplet species. In our previous work, it has been shown that the triplet state of KN is readily quenched by molecular oxygen and the tryptophan and tyrosine amino acids.[69] Consequently, the singlet oxygen and the oxidation products of tyrosine observed in the photolysis of KN-modified proteins[67,68] probably originate from the reaction of KN in the triplet state with oxygen and the tyrosine residues of proteins. Thus, alteration of the local environment may play a key role in the photochemical activity of the UV filters of the human lens.

The photochemical activity of protein-bound UV filters should probably depend on the binding site of the protein molecule.

The results of the present work show that the lifetime of the lowest singlet excited state of KN strongly depends on the ability to form intermolecular hydrogen bonds. The UV filters in the outer and inner parts of proteins have different access to solvent molecules and therefore may have different photoreactivity. It can be proposed that UV filters incorporated in the internal structure of protein produce the main damage for the lens tissue. The validation of this suggestion will be the topic of further investigations.

Conclusions

The present investigation demonstrates unambiguously that the remarkable UV-filter properties of KN arise from an ultrafast internal conversion to the ground state. The rate of internal conversion is highly sensitive to the nature of the solvent. It also depends on isotopic substitution of solvent and, to a minor degree, on temperature. It has been shown that intermolecular hydrogen bonds are responsible for the substantial acceleration of IC in protic solvents. Our results clearly point to hydrogen-bonding interactions as the dominant process in the radiationless deactivation of the lowest singlet excited state of KN.

Acknowledgment. The authors thank Dr. Omar Mohammed for the valuable remarks at the initial stages of this work as well as Dr. Alexandre Fürstenberg and Guillaume Duvanel for their help in the treatment of the fluorescence data. This work was supported by ESF DYNA Exchange Grants #1325 and #1929, by Swiss National Science Foundation grant No. 200020-115942, by Russian Foundation for Basic Research Projects 07-03-00253 and 08-03-00539, and by Grant of President RF Scientific School 3604.2008.3.

References and Notes

(1) van Heyningen, R. Fluorescent glucoside in the human lens. *Nature* **1971**, *230*, 393–394.

(2) Wood, A. M.; Truscott, R. J. W. UV filters in human lenses: tryptophan catabolism. *Exp. Eye Res.* **1993**, *56*, 317–325.

(3) Truscott, R. J. W.; Wood, A. M.; Carver, J. A.; Sheil, M. M.; Stutchbury, G. M.; Zhu, J.; Kilby, G. W. A new UV-filter compound in human lenses. *FEBS Lett.* **1994**, *384*, 173–176.

(4) Dillon, J.; Wang, R. H.; Atherton, S. J. Photochemical and photophysical studies on human lens constituents. *Photochem. Photobiol.* **1990**, *52*, 849–854.

(5) Dillon, J.; Atherton, S. J. Time resolved spectroscopic studies of the intact human lenses. *Photochem. Photobiol.* **1990**, *51*, 465–468.

(6) Krishna, C. M.; Uppuluri, S.; Riesz, P.; Zigler Jr., J. S.; Balasubramanian, D. A study of the photodynamic efficiencies of some eye lens constituents. *Photochem. Photobiol.* **1991**, *54*, 51–58.

(7) Luthra, M.; Balasubramanian, D. 3-Hydroxykynurenine and 3-Hydroxyanthranilic acid may act as endogenous antioxidants in the eye lens. *Exp. Eye Res.* **1992**, *55*, 641–643.

(8) Tsentalovich, Yu. P.; Snytnikova, O. A.; Sherin, P. S.; Forbes, M. D. E. Photochemistry of kynurenine, a tryptophan metabolite: properties of the triplet state. *J. Phys. Chem. A* **2005**, *109*, 3565–3568.

(9) Tsentalovich, Yu. P.; Snytnikova, O. A.; Forbes, M. D. E.; Chernyak, E. I. S. V.; Morozov, S. V. Photochemical and thermal reactivity of kynurenine. *Exp. Eye Res.* **2006**, *83*, 1439–1445.

(10) Sherin, P. S.; Tsentalovich, Yu.P.; Snytnikova, O. A.; Sagdeev, R. Z. Photoactivity of kynurenine-derived UV-filters. *J. Photochem. Photobiol. B: Biology* **2008**, *93*, 127–132.

(11) Lim, E. C. Proximity effect in molecular photophysics: dynamical consequences of pseudo-Jahn-Teller interaction. *J. Phys. Chem.* **1986**, *90*, 6770–6777.

(12) Wassam, W. A.; Lim, E. C. Proximity effect in radiationless transitions. *J. Chem. Phys.* **1978**, *68*, 433–454.

(13) Lai, T.-I.; Lim, B. T.; Lim, E. C. Photophysical properties of biologically important molecules related to proximity effects: psoralens. *J. Am. Chem. Soc.* **1982**, *104*, 7631–7635.

(14) Lai, T.-I.; Lim, E. C. Proximity effect and excited-state dynamics of 9-carbonyl-substituted anthracenes. *J. Am. Chem. Soc.* **1985**, *107*, 1134–1137.

(15) Sobolewski, A. L.; Domcke, W.; Dedonder-Lardeux, C.; Jouvet, C. Excited-state hydrogen detachment and hydrogen transfer driven by repulsive $1\pi\sigma^*$ states: A new paradigm for nonradiative decay in aromatic biomolecules. *Phys. Chem. Chem. Phys.* **2002**, *4*, 1093–1100.

(16) Gustavsson, T.; Banyasz, A.; Lazzarotto, E.; Markovitsi, D.; Scalmani, G.; Frich, M.; Barone, V.; Improta, R. Singlet-state behavior of uracil and thymine in aqueous solution: a combined experimental and computational study of 11 uracil derivatives. *J. Am. Chem. Soc.* **2006**, *128*, 607–619.

(17) Inoue, H.; Hida, M.; Nakashima, N.; Yoshihara, K. Picosecond fluorescence lifetimes of anthraquinone derivatives. Radiationless deactivation via intra- intermolecular hydrogen bonds. *J. Phys. Chem.* **1982**, *86*, 3184–3188.

(18) Yatsuhashi, T.; Inoue, H. Molecular mechanism of radiationless deactivation of aminoanthraquinones through intermolecular hydrogen-bonding interaction with alcohols and hydroperoxides. *J. Phys. Chem.* **1997**, *101*, 8166–8173.

(19) Yatsuhashi, T.; Nakajima, Yu.; Shimada, T.; Inoue, H. Photophysical properties of intramolecular charge-transfer excited singlet state of aminofluorenone derivatives. *J. Phys. Chem.* **1998**, *102*, 3018–3024.

(20) Oshima, J.; Yoshihara, T.; Tobita, S. Water-induced fluorescence quenching of mono- and dicyanoanilines. *Chem. Phys. Lett.* **2006**, *423*, 306–311.

(21) Oshima, J.; Shiobara, S.; Naoumi, H.; Kaneko, S.; Yoshihara, T.; Mishra, A. K.; Tobita, S. Extreme fluorescence sensitivity of some aniline derivatives to aqueous and nonaqueous environments: Mechanistic study and its implication as a fluorescence probe. *J. Phys. Chem.* **2006**, *110*, 4629–4637.

(22) Weller, A. *Naturwissenschaften* **1955**, *42*, 175. Weller, A. *Electrochem. Z.* **1956**, *60*, 1144.

(23) Van Benthem, M. H.; Gillispie, G. D. Intramolecular hydrogen bonding. 4. Dual fluorescence and Excited-State Proton Transfer in 1,5-dihydroxyanthraquinone. *J. Phys. Chem.* **1984**, *88*, 2954.

(24) Flom, S. R.; Barbara, P. F. Proton transfer and hydrogen bonding in the internal conversion of S_1 anthraquinones. *J. Phys. Chem.* **1985**, *89*, 4489–4494.

(25) Barbara, P. F.; Rentzepis, P. M.; Brus, L. E. Photochemical kinetics of salicylidenaniline. *J. Am. Chem. Soc.* **1980**, *102*, 2786–2791.

(26) Nishiya, T.; Yamauchi, S.; Hirota, N.; Baba, M.; Hanazaki, I. Fluorescence study of the intramolecularly hydrogen-bonded molecules o-hydroxyacetophenone and salicylamide and related molecules. *J. Phys. Chem.* **1986**, *90*, 5730–5735.

(27) Barbara, P. F.; Walsh, P. K.; Brus, L. E. Picosecond kinetic and vibrationally resolved spectroscopic studies of intramolecular excited-state hydrogen atom transfer. *J. Phys. Chem.* **1989**, *93*, 29–34.

(28) Fürstenberg, A.; Vauthey, E. Excited-state dynamics of the fluorescent probe Lucifer Yellow in liquid solutions and in heterogeneous media. *Photochem. Photobiol. Sci. 4* **2005**, 260–267.

(29) Mohammed, O. F.; Vauthey, E. Excited-state dynamics of nitroperylene in solution: solvent and excitation wavelength dependence. *J. Phys. Chem. A* **2008**, *112*, 3823–3830.

(30) Banerji, N.; Fürstenberg, A.; Bhosale, S.; Sisson, A. L.; Sakai, N.; Matile, S.; Vauthey, E. Ultrafast photoinduced charge separation in naphthalene diimide based multichromophoric systems in liquid solutions and in a lipid membrane. *J. Phys. Chem. B* **2008**, *112*, 8912–8922.

(31) Yoshihara, T.; Shimada, H.; Shizuka, H.; Tobita, S. Internal conversion of o-aminoacetophenone in solution. *Phys. Chem. Chem. Phys.* **2001**, *3*, 4972–4978.

(32) Shimada, H.; Nakamura, A.; Yoshihara, T.; Tobita, S. Intramolecular and intermolecular hydrogen-bonding effects on photophysical properties of 2′-aminoacetophenone and its derivatives in solution. *Photochem. Photobiol. Sci.* **2005**, *4*, 367–375.

(33) Eaton, D. F. Reference materials for fluorescence measurement. *J. Photochem. Photobiol. B: Biol.* **1988**, *2*, 523–531.

(34) Morandeira, A.; Engeli, L.; Vauthey, E. Ultrafast charge recombination of photogenerated ion pairs to an electronic excited state. *J. Phys. Chem. A* **2002**, *106*, 4833–4837.

(35) Fürstenberg, A.; Julliard, M. D.; Deligeorgiev, T. G.; Gadjev, N. I.; Vasilev, A. A.; Vauthey, E. Ultrafast excited-state dynamics of DNA fluorescent intercalators: new insight into the fluorescence enhancement mechanism. *J. Am. Chem. Soc.* **2006**, *128*, 7661–7669.

(36) Duvanel, G.; Banerji, N.; Vauthey, E. Excited-state dynamics of donor-acceptor bridged systems containing a boron-dipyrromethene chromophore: interplay between charge separation and reorientational motion. *J. Phys. Chem. A* **2007**, *111*, 5361–5369.

(37) Molokov, I. F.; Tsentalovich, Yu.P.; Yurkovskaya, A. V.; Sagdeev, R. Z. Investigation of the photo-Fries rearrangement reactions of 1- and 2-naphthyl acetates. *J. Photochem. Photobiol. A: Chem.* **1997**, *110*, 159–165.

(38) Tsentalovich, Yu. P.; Kulik, L. V.; Gritsan, N. P.; Yurkovskaya, A. V. Solvent effect on the rate of β-scission of the tert-butoxyl radical. *J. Phys. Chem. A* **1998**, *102*, 7975–7980.

(39) Lang, B.; Angulo, G.; Vauthey, E. Ultrafast solvation dynamics of coumarin 153 in imidazolium-based ionic liquids. *J. Chem. Phys. A* **2006**, *110*, 7028–7034.

(40) Fürstenberg, A.; Vauthey, E. Ultrafast excited-state dynamics of oxazole yellow DNA intercalators. *J. Phys. Chem. B* **2007**, *111*, 12610–12620.

(41) Pigliucci, A.; Duvanel, G.; Lawson Daku, L. M.; Vauthey, E. Investigation of the influence of solute-solvent interactions on the vibrational energy relaxation dynamics of large molecules in liquids. *J. Phys. Chem. A* **2007**, *111*, 6135–6145.

(42) Snytnikova, O. A.; Sherin, P. S.; Tsentalovich, Yu. P. Biphotonic ionization of kynurenine and 3-hydroxykynurenine. *J. Photochem. Photobiol. A: Chem.* **2007**, *186*, 364–368.

(43) Shin, D. N.; Wijnen, J. W.; Engberts, J. B. F. N.; Wakisaka, A. On the origin of microheterogeneity: mass spectrometric studies of acetonitrile-water and dimethyl sulfoxide-water binary mixtures (Part 2). *J. Phys. Chem. B* **2001**, *106*, 6014–6020.

(44) Taft, R. W.; Kamlet, M. J. The solvatochromic comparison method. 2. The α-scale of hydrogen-bond donor (HBD) acidities. *J. Am. Chem. Soc.* **1976**, *98*, 2886–2894.

(45) Kamlet, M. J.; Abboud, J-L.M.; Abraham, M. H.; Taft, R. W. Linear solvation relationships. 23. A comprehensive collection of the solvatochromic parameters, π^*,α and β, and some methods for simplifying the generalized solvatochromic equation. *J. Org. Chem.* **1983**, *48*, 2877–2887.

(46) *Handbook of Chemist*; Nikolsky, B. N., Ed.; State Scientific and Technical Publisher of Chemical Literature: Moscow, 1962; Vol. 1 (in Russian).

(47) Kessel, L.; Kalinin, S.; Nagaraj, R. H.; Larsen, M.; Johansson, L. B.-A. Time-resolved and steady-state fluorescence spectroscopic studies of the human lens with comparison to argpyrimidine, pentosidine and 3-OH-kynurenine. *Photochem. Photobiol.* **2002**, *76*, 549–554.

(48) Jarzeba, W.; Walker, G. C.; Johnson, A. E.; Kahlow, M. A.; Barbara, P. F. Femtosecond microscopic solvation dynamics of aqueous solutions, *J. Phys. Chem.* **1988**, *92*, 7039−7041.

(49) Jimenez, R.; Fleming, G. R.; Kumar, P. V.; Maroncelli, M. Femtosecond solvation dynamics of water. *Nature* **1994**, *369*, 471–473.

(50) Horng, M. L.; Gardecki, J. A.; Papazyan, A.; Maroncelli, M. Subpicosecond measurements of polar solvation dynamics: coumarin 153 revisited. *J. Phys. Chem.* **1995**, *99*, 17311–17337.

(51) Hassanali, A. A.; Li, T.; Zhong, D.; Singer, Sh. J. A molecular dynamics study of Lys-Trp-Lys: structure and dynamics in solution following photoexcitation. *J. Phys. Chem. B* **2006**, *110*, 10497–10508.

(52) Lim, E. C. *Excited states*; Academic Press: New York, 1977; Vol. 111, pp 305−337.

(53) Kasha, M. *Light and life*; Johns Hopkins Press: Baltimore, MD, 1961; p 31.

(54) Goodman, L.; Shull, H. A semiempirical treatment of n-π transitions. *J. Chem. Phys.* **1954**, *22*, 1138.

(55) Madej, S. L.; Okajima, S.; Lim, E. C. "Proximity effects" in radiationless transitions of aromatic molecules with nonbonding electrons: Substituent and temperature dependences of luminescence in some N-heterocyclics. *J. Chem. Phys.* **1976**, *65*, 1219.

(56) Huber, J. R.; Mahaney, M.; Morris, J. V. Temperature dependence of radiationless processes. Isoquinoline in solution. *Chem. Phys.* **1976**, *16*, 329.

(57) Lai, T.-I.; Lim, E. C. Temperature effects on $S_1 \rightarrow S_0/S_1 \rightarrow T_1$ branching ratio in radiationless transitions of N-heterocyclic compounds. *Chem. Phys. Lett.* **1979**, *62*, 507.

(58) Truscott, R. J. W. Human cataract: the mechanisms responsible; light and butterfly eyes. *Int. J. Biochem. Cell Biol.* **2003**, *35*, 1500–1504.

(59) Truscott, R. J. W. Age-related nuclear cataract - oxidation is the key. *Exp. Eye Res.* **2005**, *80*, 709–725.

(60) Taylor, L. M.; Aquilina, J. A.; Jamie, J. F.; Truscott, R. J. W. UV filter instability: consequences for the human lens. *Exp. Eye Res.* **2002**, *75*, 165–175.

(61) Aquilina, J. A.; Truscott, R. J. W. Cysteine is the initial site of modification of alpha-Crystallin by kynurenine. *Biochem. Biophys. Res. Commun.* **2000**, *276*, 216–223.

(62) Aquilina, J. A.; Truscott, R. J. W. Identifying sites of attachment of UV filters to proteins in older human lenses. *Biochim. Biophys. Acta* **2002**, *1596*, 6–15.

(63) Garner, B.; Shaw, D. C.; Lindner, R. A.; Carver, J. A.; Truscott, R. J. W. Non-oxidative modification of lens crystallins by kynurenine: a novel post-translational protein modification with possible relevance to ageing and cataract. *Biochim. Biophys. Acta* **2000**, *1476*, 265–278.

(64) Kopylova, L. V.; Snytnikova, O. A.; Chernyak, E. I.; Morozov, S. V.; Tsentalovich, Yu. P. UV filter decomposition. A study of reactions of 4-(2-amino-3-aminophenyl)-4-oxocrotonic acid with amino acids and antioxidants present in the human lens. *Exp. Eye Res.* **2007**, *85*, 242–249.

(65) Lerman, S.; Borkman, R. Spectroscopic evaluation and classification of the normal, aging and cataractous lens. *Ophthal. Res.* **1976**, *8*, 335–353.

(66) Yu, N. T.; Barron, C. B.; Kuck, J. F. R. Distribution of two metabolically related fluorophors in human lens measured by laser microprobe. *Exp. Eye. Res.* **1989**, *49*, 189–194.

(67) Parker, N. R.; Jamie, J. F.; Davies, M. J.; Truscott, R. J. W. Protein-bound kynurenine is a photosensitiser of oxidative damage. *Free Radical Biol. Med.* **2004**, *37*, 1479–1489.

(68) Mizdrak, J.; Hains, P. G.; Truscott, R. J. W.; Jamie, J. F.; Davies, M. J. Tryptophan-derived ultraviolet filter compounds covalently bound to lens proteins are photosensitizers of oxidative damage. *Free Radical Biol. Med.* **2008**, *44*, 1108–1119.

(69) Snytnikova, O. A.; Sherin, P. S.; Kopylova, L. V.; Tsentalvich, Yu. P. Kinetics and mechanism of reactions of photoexcited kynurenine with molecules of some natural compounds. *Russ. Chem. Bull.* **2007**, *56*, 732–738.

JP900541B